de Meis, L., de Souza Otero, A., Martins, O. B., Alves, E. W., Inesi, G., & Nakamoto, R. (1982) *J. Biol. Chem. 257*, 4993–4998.
de Souza Otero, A., & de Meis, L. (1982) *Z. Naturforsch. C: Biosci. 37C*, 527–531.
Dupont, Y. (1980) *Eur. J. Biochem. 109*, 231–238.
Dupont, Y. (1982) *Biochim. Biophys. Acta 688*, 75–87.
Epstein, M., Kuriki, Y., Biltonen, R., & Racker, E. (1980) *Biochemistry 19*, 5564–5568.
Guillain, F., Gingold, M. P., Büschlen, S., & Champeil, P. (1980) *J. Biol. Chem. 255*, 2072–2076.
Guillain, F., Gingold, M. P., & Champeil, P. (1982) *J. Biol. Chem. 257*, 7366–7371.
Guimaraes-Motta, H., & de Meis, L. (1980) *Arch. Biochem. Biophys. 203*, 395–403.
Hackney, D. D., Stempel, K. E., & Boyer, P. D. (1980) *Methods Enzymol. 64*, 60–83.
Ikemoto, N., Miyao, A., & Kurobe, Y. (1981) *J. Biol. Chem. 256*, 10809–10814.
Inesi, G., Watanabe, T., Coan, C., & Murphy, A. (1982) *Ann. N.Y. Acad. Sci. 402*, 515–534.
Inesi, G., Lewis, D., & Murphy, A. (1984) *J. Biol. Chem. 259*, 996–1003.
Kanazawa, T. (1975) *J. Biol. Chem. 250*, 113–119.
Kanazawa, T., & Boyer, P. D. (1973) *J. Biol. Chem. 248*, 3163–3172.
Knowles, A. F., & Racker, E. (1975) *J. Biol. Chem. 250*, 1949–1951.
Kolassa, N., Punzengruber, C., Suko, J., & Makinose, M. (1979) *FEBS Lett. 108*, 495–500.
Lacapère, J. J., Gingold, M. P., Champeil, P., & Guillain, F. (1981) *J. Biol. Chem. 256*, 2302–2306.
Loomis, C. R., Martin, D. W., Mc Caslin, D. R., & Tanford, C. (1982) *Biochemistry 21*, 151–156.
Martin, D. W., & Tanford, C. (1981) *Biochemistry 20*, 4597–4602.
Masuda, H., & de Meis, L. (1973) *Biochemistry 12*, 4581–4585.
Masuda, H., & de Meis, L. (1977) *J. Biol. Chem. 252*, 8567–8571.
McIntosh, D. B., & Boyer, P. D. (1983) *Biochemistry 22*, 2867–2875.
Murphy, A. J., Pepitone, M., & Highsmith, S. (1982) *J. Biol. Chem. 257*, 3551–3554.
Punzengruber, C., Prager, R., Kolassa, N., Winkler, F., & Suko, J. (1978) *Eur. J. Biochem. 92*, 349–359.
Rauch, B., Von Chak, D., & Hasselbach, W. (1977) *Z. Naturforsch. C: Biosci. 32C*, 828–834.
Shigekawa, M., Dougherty, J. P., & Katz, A. M. (1978) *J. Biol. Chem. 253*, 1442–1450.
Takisawa, H., & Makinose, M. (1981) *Nature (London) 290*, 271–273.
Vieyra, A., Scofano, H. M., Guimaraes-Motta, H., Tume, R. K., & de Meis, L. (1979) *Biochim. Biophys. Acta 568*, 437–445.
Watanabe, T., Lewis, D., Nakamoto, R., Kurzmack, M., Fronticelli, C., & Inesi, G. (1981) *Biochemistry 20*, 6617–6625.

Electron-Transfer Reactions of Photoreduced Flavin Analogues with *c*-Type Cytochromes: Quantitation of Steric and Electrostatic Factors†

T. E. Meyer, J. A. Watkins, C. T. Przysiecki, G. Tollin, and M. A. Cusanovich*

ABSTRACT: We have found correlations between rate constants and the difference in redox potential of the reactants for electron-transfer reactions between oxidized cytochromes and either photoproduced riboflavin or flavin mononucleotide (FMN) semiquinones (the latter rate constants extrapolated to infinite ionic strength). The riboflavin–cytochrome rate constants are about 70% of those for reduction by lumiflavin, probably because of steric interference by the ribityl side chain. Reduction of cytochromes by FMN semiquinone was ionic strength dependent in all cases, due to electrostatic interactions. Extrapolation of rate constants to infinite ionic strength shows that the phosphate exerts a significant steric effect as well (rate constants average about 27% of those for lumiflavin, although part of this decrease is due to a difference in the semiquinone p*K* value). Differences in the magnitude of the FMN steric effect correlate well with surface topology differences for those cytochomes whose three-dimensional structures are known. Mitochondrial cytochromes *c* and the cytochromes c_2 all showed attractive (plus–minus) interaction with FMN in spite of the fact that some of these proteins have large net negative charges. Four small *c*-type cytochromes (including *Pseudomonas* cytochrome *c*-551) show a weak repulsive interaction with FMN semiquinone. We conclude that flavosemiquinones interact at a site on the cytochromes that is near the exposed heme edge. There is a large positive electrostatic field at this site in mitochondrial cytochrome *c* and the cytochromes c_2, but this region is primarily hydrophobic in *Pseudomonas* cytochrome *c*-551 and in the other small bacterial cytochromes. In the *Pseudomonas* reaction, FMN interacts weakly with a negative electrostatic field, which must be somewhat removed from the site of electron transfer. The relative contributions of redox potential, steric effects, and electrostatic interactions for the flavosemiquinone–cytochrome reactions described herein are roughly equivalent and correspond to rate constant changes of 2–5-fold.

We have been using flavin semiquinones generated by laser flash photolysis as reductants to study electron-transfer mechanisms in cytochromes and other redox proteins (Ahmad et al., 1981; Meyer et al., 1983). Theoretically, one would expect that redox potentials, steric factors, and electrostatics should all contribute to rate constants for the reaction, but until recently, the quantitative contributions of these factors have not been demonstrated. By using a large set of homologous

† From the Department of Biochemistry, University of Arizona, Tucson, Arizona 85721. *Received March 9, 1984.* This work was supported in part by grants from the National Institutes of Health, AM 15057 (G.T.) and GM 21277 (M.A.C.).

0006-2960/84/0423-4761$01.50/0

cytochromes, which differ by nearly 500 mV in redox potential and are so divergent in amino acid sequence as to preclude a unique alignment of their peptide chains, we were able to show a correlation between rate constants and redox potential differences for reduction by the neutral lumiflavin semiquinone (Meyer et al., 1983). We now report on the effects of steric and electrostatic factors with riboflavin and FMN semiquinones as reductants.

It is well-known that physiological electron-transfer reactions involving mitochondrial cytochrome *c* involve a large electrostatic component. In recent years, a variety of approaches have established that the site of electron transfer is near the solvent-exposed edge of the heme, which is surrounded by lysine residues (Salemme et al., 1973; Miller & Cusanovich, 1974; McArdle et al., 1974, Staudenmayer et al., 1977, Ferguson-Miller et al., 1978; Rieder & Bosshard, 1980; Smith et al., 1980). These studies, utilizing the strongly cationic mitochondrial cytochrome *c* protein molecule, have focused on electrostatic interactions and have led to proposals concerning the role of protein net charge and protein dipole moment in influencing electron-transfer kinetics (Koppenol & Margoliash, 1982). However, in some cases it has been argued that the local environment at the site of electron transfer and not the net protein charge is the important parameter (Wood et al., 1977; Smith et al., 1981; Rickle & Cusanovich, 1979; Simondsen et al., 1982). More importantly, most studies to date have not addressed the role of steric effects and oxidation–reduction potentials in the kinetics of electron transfer by *c*-type cytochromes.

There is now available a large body of structural information on other *c*-type cytochromes that have physicochemical and structural properties quite distinct from respiratory cytochrome *c*. These include the bacterial cytochromes c_2,[1] which are the nearest homologues of the mitochondrial cytochromes *c* (Meyer & Kamen, 1982) and which, despite also having lysine residues close to the heme edge, have oxidation–reduction potentials varying from 250 to 470 mV and isoelectric points that range from basic to neutral to acidic. In addition, there are smaller and structurally more divergent bacterial cytochromes that exhibit an even wider range of physicochemical properties. The best known of these, *Pseudomonas* cytochrome *c*-551, has a nearly uniform charge distribution with neutral side chains close to the exposed heme edge (Matsuura et al., 1982). Thus, the available cytochromes offer the opportunity to investigate the relative contribution of localized vs. net protein charge to electrostatic interactions during electron transfer. Moreover, because of the differences in surface topology among these proteins, the possibility also exists that information concerning the relative role of steric interactions can be obtained.

The studies reported here make use of a wide range of homologous *c*-type cytochromes and a series of reduced flavins to provide further insight into the mechanism of electron transfer. Specifically, rate constants for reduction by the semiquinone forms of lumiflavin, riboflavin, and FMN have been compared. Lumiflavin semiquinone is an uncharged small reductant[2] that should be uninfluenced by electrostatic forces. Riboflavin semiquinone also has no net charge but has a ribityl side chain in place of a methyl group attached to the N10 position of the isoalloxazine ring. FMN, which is riboflavin 5′-phosphate, can provide information on the role of both electrostatic and steric interactions, the latter being resolvable by extrapolation of rate constant data to infinite ionic strength at which point all electrostatic factors are presumably no longer important. As we will demonstrate below, these studies have allowed us to obtain quantitative information on the magnitude of these effects and thus to provide a model for future investigation of the factors that control electron-transfer rates of redox proteins.

Experimental Procedures

The laser flash photolysis apparatus, techniques, and data analysis were as described previously (Simondsen & Tollin, 1983; Ahmad et al., 1981; Meyer et al., 1983). Sources of protein were also as previously published (Meyer et al., 1983). First-order decay of flavin radical and appearance of reduced cytochrome was followed at 575 nm (typical cytochrome Δ extinction, -3 mM^{-1} cm^{-1}) under anaerobic conditions over three to four half-lives. This wavelength was chosen so that a net loss of absorbance resulted on cytochrome reduction, which simplifies data analysis. Protein concentrations were varied over a 5–10-fold range with minimum concentrations of about 5 μM and maximum of about 100 μM. The lower range was determined by the relative rates of flavin disporportionation and protein reduction and the upper range by loss of signal due to excitation light absorption by the cytochrome. Typically, five to six concentrations were sufficient for the determination of second-order rate constants. No saturation effects were observed (i.e., all second-order plots were linear). FMN was purified under dim light by passage through a Biogel P-2 gel filtration column equilibrated with double-distilled water (Nagy et al., 1982) and lyophilized. Solutions were made up immediately prior to use. Standard buffer solutions containing 60 μM flavin, 10 mM ethylenediaminetetraacetic acid (EDTA), and 20 mM sodium phosphate, pH 7.0, were used for the lumiflavin and riboflavin experiments. The 16 mM ionic strength buffer contained 1 mM EDTA and 5 mM phosphate. Higher ionic strengths were made up with 10 mM EDTA and 20, 52, 100, and 222 mM phosphate, pH 7.0, giving ionic strengths of 96, 160, 256, and 500 mM, respectively. Ionic strengths of 160 and 500 mM were also made up with standard buffer plus sodium chloride to test for specific ion effects (there was no effect with tuna cytochrome *c*).

Protein net charge was calculated by adding negative charges due to Glu and Asp side chains and the two heme propionates and by adding positive charges due to Lys and Arg side chains and heme iron. Although in individual proteins the propionates may have ionization constants near pH 7, this was not considered in the calculation. Histidine residues, excluding the ligated histidine, were assumed to have an ionization constant equal to that for free histidine, i.e., pK = 6, and fractional charges were calculated on this basis. Blocked N-termini added one negative charge.

Protein dipole moments were calculated as described by Koppenol & Margoliash (1982). Coordinates of amino- and carboxyl-terminal residues and heme iron were included. It was found that treating the heme propionates as having either charged or uncharged carboxyls had no significant effect on the calculated dipole moments (<10%). Histidine residues were included as described in the previous paragraph.

In order to estimate the rate constants for cytochrome reduction by FMN semiquinone at infinite ionic strength (k_∞) and the charge of the cytochrome interaction domain (Z_1), eq 1 was used (Watkins, 1984), where $X(I)$, $Y(I)$, and $Z(I)$

[1] *Paracoccus denitrificans* cytochrome *c*-550 is classified as a cytochrome c_2 on the basis of sequence homology and three-dimensional structure (Meyer & Kamen, 1982).

[2] More accurately, the neutral semiquinones of lumiflavin and riboflavin (pK = 8.36) are zwitterionic; at pH 7.0, approximately 4% of the semiquinone is in the anionic form.

$$\ln k(I) = \ln k_\infty - V_{ii}X(I) - V_{id}Y(I) - V_{dd}Y(I)^2Z(I) \quad (1)$$

are ionic strength (I) dependent parameters (see legend to Table I) and V_{ii}, V_{id}, and V_{dd} are the electrostatic energies due to ion–ion, ion–dipole, and dipole–dipole interactions, respectively.

Equation 1 was derived by treating the interaction domains of the reactants as parallel disks (with radius ρ) having a discrete point charge (Z_1 and Z_2) equivalent to the net charge of the interaction domain defined by ρ (Watkins, 1984). The influence of the protein dipole moment on the electrostatics of the interaction domain is included in both the ion–dipole and dipole–dipole terms (see legend to Table I). The details of this model and of the derivation of the equations will be described elsewhere.

V_{ii} is given by eq 2, where $\alpha = e^2/(2\pi kT)$ ($\alpha = 128.47$),

$$V_{ii} = D_e^{-1}\alpha Z_1 Z_2 r_{12}\rho^{-2} \quad (2)$$

D_e is the effective dielectric constant at the site of interaction (estimated to be 50, assuming some exclusion of water from the interaction domain on formation of the transition state), Z_1 is the charge at the cytochrome interaction site, Z_2 is the charge on FMN (−1.9 at pH 7.0), and r_{12} is the distance in angstroms between reactants when electron transfer occurs (taken as 3.5 Å, van der Waals radius).

It is important to note that analysis of the data by the approach developed by Wherland and Gray (1976) based on Debye and Marcus theory yields parallel results for the values of k_∞. Specifically, the k_∞ values obtained from eq 1 and reported below are typically 65% of those determined from the Wherland–Gray equation. Thus, the conclusions that can be drawn from the relative values of k_∞ are independent of the electrostatic model used, although the absolute values of k_∞ will be model dependent. The Wherland–Gray approach, derived from a point-charge model, requires use of the net protein charge and does not provide information on active site charges.

For the reaction of FMN semiquinone with c-type cytochromes of known structure, for which the dipole moments can be calculated, we find that V_{dd} is negligible and V_{id} contributes 10–35% of the interaction energy. For the analysis of the electrostatic interaction with cytochromes of unknown structure, experimental data (rate constants as a function of ionic strength) were analyzed in terms of eq 1 by using a steepest descents procedure to obtain estimates of V_{ii}, ρ, and k_∞. Given ρ and V_{ii}, eq 2 can be used to calculate Z_1 by using a value of −1.9 for Z_2.

Results and Discussion

In a previous investigation of electron-transfer reactions between lumiflavin semiquinone and a series of homologous cytochromes (Meyer et al., 1983), it was found that rate constants could be related to the differences in redox potential between the reactants by using semiempirical free-energy equations developed by Rehm & Weller (1969) and by Marcus (1968) and Agmon & Levine (1977). We also found a similar relationship for reaction between lumiflavin semiquinone and high-potential iron–sulfur proteins (HiPIP's). The cytochromes were intrinsically more reactive than HiPIP's at the same redox potential, which was attributed to the relative degree of exposure of the redox centers. The intrinsic reactivity of other nonrelated heme proteins, iron–sulfur proteins, and copper proteins could also be qualitatively related to the relative steric inaccessibility of the redox centers. If proteins with buried redox centers react more slowly with lumiflavin semiquinone than do those with more exposed centers, then

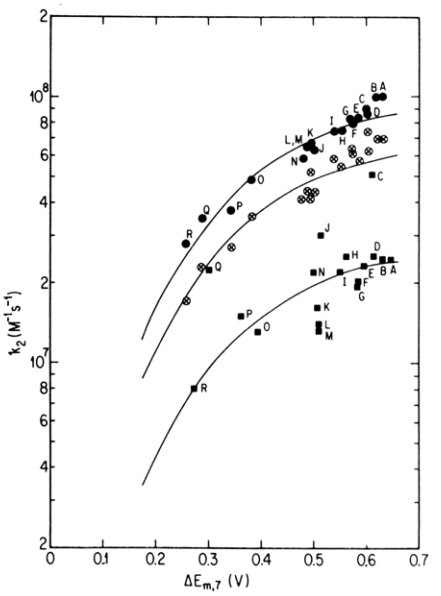

FIGURE 1: Plot of calculated second-order rate constants for reduction of c-type cytochromes by flavin semiquinones vs. difference in redox potential. Solid lines are theoretical curves based on the Marcus exponential equation, which relates activation free energy (ΔG^+) and thermodynamic free energy ($\Delta G°$) (see text) with parameters as defined below: $\Delta G^\ddagger = \Delta G° + [\Delta G^\ddagger(0)/\ln 2] \ln (1 + \exp[(\Delta G° \ln 2)/\Delta G^\ddagger(0)])$, where $\Delta G^\ddagger(0)$ = intrinsic barrier (energy required to reach transition state when $\Delta G° = 0$) and $k_2 = \nu_{ET} \exp(-[\Delta G^\ddagger/(RT)])$, where ν_{ET} is the limiting rate constant as $\Delta G°$ approaches infinity. (●) Lumiflavin; $\nu_{ET} = 1 \times 10^8$ M^{-1} s^{-1} and $\Delta G^\ddagger(0) = 2.75$ kcal/mol; with the exception of proteins labeled as C, E, F, I, K, L (tuna), and O, data are from Meyer et al. (1983). (⊗) Riboflavin; $\nu_{ET} = 0.7 \times 10^8$ M^{-1} s^{-1} and $\Delta G^\ddagger(0) = 2.75$ kcal/mol. (■) FMN; $\nu_{ET} = 0.27 \times 10^8$ M^{-1} s^{-1} and $\Delta G^\ddagger(0) = 2.75$ kcal/mol. Points correspond to rate constants extrapolated to infinite ionic strength. (A) *Rhodopspirillum tenue* 3761 *c*-553; (B) *Rhodopspirillum tenue* 2761 *c*-553; (C) *Euglena* sp. *c*-552; (D) *Rhodopseudomonas spheroides* c_2; (E) *Rhodomicrobium vanniellii* c_2; (F) *Rhodopseudomonas capsulata* c_2; (G) *Rhodocyclus purpureus c*-553; (H) *Rhodospirillum rubrum* c_2; (I) *Rhodospirillum salexigens* c_2; (J) *Pseudomonas aeruginosa c*-551; (K) *Candida krusei c*; (L) tuna *c*; (M) horse *c*; (N) *Paracoccus dentrificans* c_2; (O) *Chlorobium thiosulfatophilum c*-555; (P) halophilic *Paracoccus* sp. *c*-554(548); (Q) *Ectothiorhodospira halophila c*-551; (R) *Rhodopseudomonas gelatinosa c*-550.

flavins more bulky than lumiflavin should also react more slowly with the homologous series of cytochromes. Second-order rate constants for the reactions of 18 cytochromes and photoproduced riboflavin semiquinone are plotted vs. the difference in redox potential between reactants in Figure 1. Data for lumiflavin semiquinone are also included for comparison. It is evident that the riboflavin rate constants correlate with redox potential differences in a manner analogous to that of lumiflavin, although the rate constants are uniformly smaller. The solid lines in Figure 1 are calculated theoretical curves from the exponential equation developed by Marcus (1968) and Agmon & Levine (1977). The lumiflavin curve is a least-squares fit to the data points, whereas the riboflavin curve was calculated by arbitrarily assuming the same intrinsic barrier [$\Delta G^\ddagger(0)$] as found for lumiflavin. The riboflavin–cytochrome limiting rate constant (ν_{ET}) is approximately 70% that of the lumiflavin–cytochrome reactions. We attribute this decrease to a steric effect of the bulky ribityl side chain.[3] Przysiecki (1984) has found that the flavin anion radical is more reactive than is the neutral radical for reactions of both lumiflavin and riboflavin with HiPIP's and cytochromes.

[3] This conclusion is different from that of Ahmad et al. (1981). We attribute this to an error in the earlier measurement.

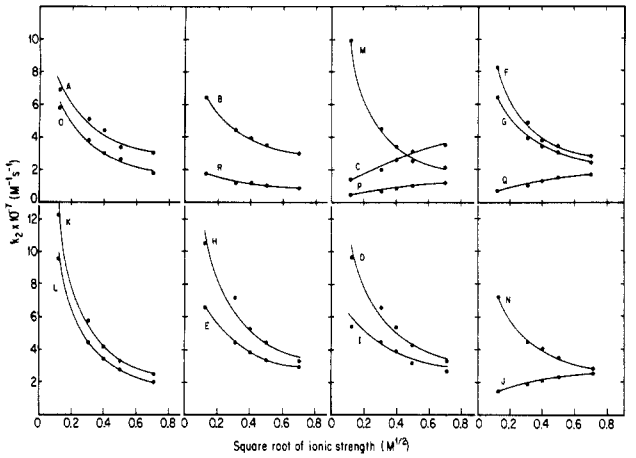

FIGURE 2: Plots of second-order rate constants for reduction of cytochromes by FMN semiquinone vs. square root of ionic strength. Curves are labeled the same as in Figure 1. Solid lines are theoretical from eq 1 and neglecting V_{id} and V_{dd} (see text for details).

However, since lumiflavin and riboflavin have the same semiquinone pK values (Vaish & Tollin, 1971; Przysiecki, 1984), this cannot be a contributing factor to the observed difference in reactivity at pH 7. This result is consistent with our earlier suggestion (Meyer et al., 1983) of a correlation between exposure of redox centers and intrinsic reactivity. Presumably, the ribityl side chain of riboflavin makes it sterically more difficult for the isoalloxazine ring to approach the heme edge of the cytochrome, thus increasing the average distance over which electron transfer must occur. On the basis of the correlation shown in Figure 1, we can conclude that this results in an average decrease in rate constant of 30% for the cytochromes studied.

Electron-transfer reactions between cytochromes and ionic oxidants and reductants, such as the iron hexacyanides, are known to be electrostatically controlled (Miller & Cusanovich, 1975; Wood et al., 1977). The reactions between the homologous cytochromes and the net negatively charged FMN radical also show an ionic strength dependence characteristic of electrostatic interactions (control experiments with riboflavin showed no ionic strength dependence). Rate constants are plotted vs. the square root of ionic strength in Figure 2. The solid lines represent theoretical fits to the data by the treatment of Watkins (1984) (see Experimental Procedures). From the slopes of the ionic strength dependence of the rate constants, it is immediately apparent that there are both plus–minus and minus–minus interactions between FMN and the cytochromes and that there is no strict correlation between the sign of the interaction and the net protein charge (cf. Table II). Thus, the net charge of *Rhodospirillum rubrum* cytochrome c_2 is 0, of *Rhodopseudomonas spheroides* cytochrome c_2 is 2–, of *Rhodospirillum salexigens* cytochrome c_2 is 5–, and of *Paracoccus* cytochrome c_2 is 7–, whereas all of the cytochromes c_2, as well as the net positively charged mitochondrial cytochromes c, show a plus–minus interaction with FMN. This indicates either that FMN semiquinone reacts at a specific site on the protein and experiences a very localized electrostatic field or that a protein dipole moment arising from asymmetrically distributed charges plays a major role in orienting the proteins for reaction. It is well-known from X-ray crystallography that the charged amino acid side chains are asymmetrically distributed in the cytochromes c_2 as well as in mitochondrial cytochrome c. Thus, Salemme et al. (1973) showed that *Rs. rubrum* cytochrome c_2 has several positively charged lysine side chains near the exposed edge of the heme, and Timkovich & Dickerson (1976) found that *Paracoccus*

Table I: Contribution of Ion–Ion and Ion–Dipole Interactions

cytochrome	total interaction energy [V_0 (kcal/mol)] calcd[a]	fitted[b]	% V_{ii}	% V_{id}
cytochrome c, tuna	−3.1	−2.9	87	13
cytochrome c, horse	−3.2	−3.0	89	11
cytochrome c_2, *Rs. rubrum*	−2.4	−2.2	85	15
cytochrome c_2, *Pr. denitrificans*	−2.1	−1.8	73	27
cytochrome c-551, *Ps. aeruginosa*	0.8	1.1	135	35[c]
cytochrome c-555, *Ch. thiosulfatophilum*	−2.2	−2.2	93	7

[a] Calculated from $V_0 = V_{ii} + V_{id} + V_{dd}$, where V_{ii} is given by eq 2, $V_{id} = \alpha D_{id}^{-1}[Z_1\mu_2^0(\cos\theta_2)(r_{12} + R_2)^{-2} + Z_2\mu_1^0(\cos\theta_1)(r_{12} + R_1)^{-2}]$, and $V_{dd} = \alpha D_{dd}^{-1}\mu_1^0\mu_2^0(\cos\theta_{12})(r_{12} + R_1 + R_2)^{-3}$. R_1 and R_2 are the full radii of the cytochrome and FMN (8 Å), θ_1 is the angle between the dipole moment vector and the sulfur of cysteine-17, θ_2 is the angle between the dipole moment vector and the 8α-methyl group of FMN, μ_1^0 is the dipole moment of the cytochrome, and μ_2^0 is the dipole moment of FMN (the average of six conformations was used). $\theta_{12} = 180 - (\theta_1 - \theta_2)$, $D_{id} = 42.8$, $D_{dd} = 44.3$, and α and r_{12} are as defined previously. [b] From analysis of the experimental data with eq 1, where $X(I) = (1 + \kappa\rho)^{-1}\exp(-\kappa\rho)$, $Y(I) = \kappa(1 + \beta)(1 + \kappa\rho)^{-1} + [1 + \kappa^2\rho^2/3 + \kappa\rho(n^2 + 2)/6]^{-1}$, $Z(I) = [1 + \kappa\rho + \kappa^2\rho^2/3 + \kappa^2(\rho + 1.5)^2/(6\rho)]^{-1}\exp(-\kappa\rho)$. $\kappa = 0.3295I^{1/2}$, $\beta = D_s(n^2 + 2)n^{-2}(2D_s + D_i)^{-1}$ (where D_s is the surface dielectric constant, taken as 50, D_i is the internal dielectric constant, which is taken as 5, and n is the internal index of refraction, $n^2 = 2.4$), and ρ = radius of the interaction domain as defined in the text. [c] For this cytochrome, the ion–ion term was repulsive (1.0 kcal/mol) whereas the ion–dipole term was attractive (−0.35 kcal/mol).

cytochrome c_2 also has positive charges near the heme edge. In both cases, the negative charges are mainly located in the other hemisphere. Van Leeuwen (1983) concluded that in situations where ionic strength studies indicate that the sign of the charge product (i.e., the slope of the rate constant vs. ionic strength curve) is opposite to that expected from net protein charge, dipole interactions are likely to be important. In order to investigate this possibility, we made use of the electrostatic model described above along with X-ray crystal structure information.

Attempts to fit eq 1 to the rate constant data for individual cytochromes as a function of ionic strength with FMN semiquinone as the reductant gave the best least-squares errors when little or no contribution from the V_{id} or V_{dd} term was included. This suggests that the dominant contribution to the interaction energy is due to the V_{ii} term. In order to test this, we analyzed the data for six cytochromes (see Table I) for which atomic coordinates are available and, thus, for which estimates of V_{id} and V_{dd} can be made. Since the dipole moment of FMN is small (~17 D), the V_{dd} term was negligible in all cases. V_{id} was calculated from the equation given in the legend to Table I, with Z_1 as the only experimentally required parameter. The other terms (μ_2, cos θ_2, μ_1, cos θ_1, r_{12}, R_2, R_1, and Z_2) either were known or were calculated from the appropriate atomic coordinates and are defined in the legend to Table I. The values of Z_1 used in the calculation are given in Table II. They were obtained from eq 2 by fitting the experimental data to eq 1 to obtain V_{ii} and ρ as described under Experimental Procedures. Although this approach is indirect, it is a reasonable first approximation since, as mentioned above, the attempts to fit eq 1 to the data including all the interactions indicated that the V_{ii} term was dominant. V_{ii} can also be calculated from eq 2 by using the above values for Z_1 and ρ. The total "calculated" interaction energy and % V_{ii} and % V_{id} given in Table I were estimated in this way. The "fitted" interaction energies given in Table I are the V_{ii} values obtained from the data fits as described above. It is important to note that if net protein charge (for Z_1) and full protein radius (for

Table II: Effect of Ionic Strength on the Reaction of *c*-Type Cytochromes with FMN

cytochrome source	E_m (pH 7) (mV)	ρ	V_{ii} (kcal/mol)	Z_1	$k_\infty \times 10^7$ (M^{-1} s^{-1})	net protein charge
Rs. tenue 3761	400	4.5	−1.6	2.1	2.4	4+
Rs. tenue 2761	390	4.5	−1.5	1.7	2.4	5+
Euglena sp.	370	4.0	+1.8	−1.7	5.2	8−
Rh. spheroides	370	4.5	−2.0	2.4	2.5	2−
Rm. vanniellii	354	4.5	−1.5	1.8	2.3	2+
Rh. capsulata	350	5.0	−2.1	3.1	2.0	1+
Rc. purpureus	340	4.5	−1.7	2.0	1.9	5+
Rs. rubrum	324	4.5	−2.2	1.9	2.5	0
Rs. salexigens	314	4.0	−1.3	1.3	2.2	5−
Ps. aeruginosa	270	5.0	+1.1	−1.1	3.0	2−
Cn. krusei	265	5.0	−3.0	4.7	1.6	5+
tuna	260	5.0	−2.9	3.0	1.4	7+
horse	260	5.0	−3.0	3.1	1.3	7+
Pr. denitrificans	250	4.5	−1.8	1.5	2.2	7−
Ch. thiosulfatophilum	150	4.0	−2.2	1.4	1.3	6+
halophilic *Paracoccus* sp.	114	5.0	+1.7	−2.5	1.5	7−
Ec. halophila	58	5.0	+1.7	−2.5	2.2	10−
Rh. gelatinosa	28	4.5	−1.2	1.5	0.8	5+

ρ) are used, the experimental data could not be adequately fit. Table II summarizes the values of ρ, Z_1, and k_∞ obtained from fitting the data given in Figure 2.

In Figure 2, the solid lines are from fits of the experimental data with eq 1 and the values of Z_1, ρ, and V_{ii} given in Table II. As can be seen, the fits are quite adequate. For reference, the midpoint potential and net charge on each cytochrome are also listed in Table II. The values of ρ were fitted to the nearest 0.5 Å and fall in the range of 4–5 Å for all the cytochromes studied. This is not unreasonable for an interaction site involving the region in the vicinity of the heme edge. In most cases, Z_1 is substantially less than the net protein charge. Most striking are those cytochromes that have a net protein charge with a sign different from the apparent interaction site charge and those in which the net charge is smaller than the interaction site charge (e.g., *Rh. spheroides*, *Rhodopseudomonas capsulata*, and *Rs. rubrum*). In four cases (*Pseudomonas aeruginosa*, *Euglena* sp., the halophilic *Paracoccus* sp. and *Ectothiorhodospira halophila*) the net protein charge and interaction site charge are both negative, although for only one of these are they the same size (*Ps. aeruginosa*). The values of Z_1, reported in Table II for cytochromes of known structure, are not unreasonable for a reaction occurring in the vicinity of the heme edge on the basis of analogy to the proposed interaction domain for the flavodoxin–cytochrome *c* complex (Simondsen et al., 1982). Using the same region of the surface, we would expect interaction domain charges of 4+ for the horse, tuna, *Paracoccus denitrificans*, and *Rs. rubrum* cytochromes as compared to the values of 3.1+, 3.0+, 1.5+, and 1.9+ found (Table II). Similarily, we expect interaction domain charges of 1+ and 2+ for the *Ps. aeruginosa* and *Chlorobium thiosulfatophilum* cytochromes, respectively, as compared to 1.1− and 1.4+ that were found. Considering that FMN has a smaller radius than flavodoxin (4.5–5 Å vs. 7.2 Å) and would thus be expected to interact with a smaller number of charged groups, this is satisfactory agreement, with the exception of *Ps. aeruginosa* cytochrome *c*-551 (see below). Our supposition that a localized region of the cytochrome surface is primarily responsible for the observed electrostatic interactions is similar to previous proposals (Miller & Cusanovich, 1975; Wood et al., 1977; Rickle & Cusanovich, 1979; Smith et al., 1981; Simondsen et al., 1982) although derived in a different way. Although the dipole moment plays a significant role in its contribution to the ion–dipole interaction, it is not the sole determinant of reactivity.

The above considerations are all consistent with the conclusion that FMN reacts at a specific site on the protein and experiences a very localized electrostatic field. We believe that site to be the exposed edge of the heme with the electrostatic field at the site of electron transfer for each of the cytochromes dependent on the specific distribution of charged residues (Matthew et al., 1983). In the net negatively charged cytochromes c_2, the positive electrostatic field at the heme edge is smaller than that in the mitochondrial cytochromes. The presumed electron-transfer site in *Pseudomonas* cytochrome *c*-551 is primarily hydrophobic, yet FMN interacts with a negatively charged site. Presumably, uncompensated negatively charged residues in the vicinity of the site of electron transfer, such as residues 68–70 (Asp-Asp-Glu), create a negative electrostatic field that can be detected by the FMN phosphate group.

The values of k_∞ have been plotted against redox potentials in Figure 1. It should be noted that, as was the case with riboflavin, the FMN rate constants (for most of the cytochromes) are again uniformly decreased in magnitude. The rate constants for the reaction of the various cytochromes with FMN semiquinone at infinite ionic strength are expected to be smaller than those with lumiflavin semiquinone on two grounds. First, due to the presence of the ribityl side chain in FMN, at least a 30% decrease in rate constant is expected, as was found for riboflavin semiquinone. Second, the pK of the FMN semiquinone is 8.6 as compared to 8.3 for lumiflavin and riboflavin semiquinones (Draper & Ingraham, 1968; Vaish & Tollin, 1971). Hence, a lower concentration of the more reactive anion semiquinone will be present at pH 7.0. To sort out these two effects, the FMN semiquinone reduction kinetics for both *Ps. aeruginosa* and horse heart cytochrome *c* were investigated as a function of pH (at I = 161 mM). In both cases it was found that the rate constant for FMN semiquinone reduction at pH 7 was 80% of that expected if the pK was 8.3 instead of 8.6. Thus, after correction for both the pK and steric effects, the FMN semiquinone rate constant should be 56% of the lumiflavin semiquinone rate constant (0.7 × 0.8 × 100). In fact, we observed rate constants that averaged about 27% of those for lumiflavin semiquinone, suggesting that the phosphate group exerts a significant steric effect as well.

In the plot of FMN–cytochrome rate constants (k_∞) vs. redox potentials in Figure 1, it can be seen that 12 cytochromes, including *Paracoccus* cytochrome c_2 and *Rs. rubrum* cytochrome c_2, lie close to the theoretical curve but that the three mitochondrial cytochromes *c* fall significantly below it and that *Pseudomonas*, *Ectothiorhodospira*, and *Euglena* cytochromes are well above it. This indicates that there may be a difference in the steric interactions with the latter six

Table III: Correlation between Cytochrome–FMN Semiquinone Reactivity and Distance of the Heme from the Protein Surface[a]

cytochrome	FMN reactivity ratio	distance of heme from surface (Å)
Euglena	2.30	*b*
Ectothiorhodospira	2.30	*b*
Pseudomonas	1.50	0.03
Rs. rubrum	1.14	0.2
Paracoccus	1.10	0.5
Candida	0.80	1.5[c]
tuna	0.65	1.8
horse	0.65	1.8[c]

[a] FMN reactivity ratio of cytochromes is defined as the ratio of experimental (data points in Figure 1) to theoretical rate constants (solid line in Figure 1). The distance from the protein surface to the edge of the heme was determined by measuring the perpendicular distance from the heme β-methyl to the plane formed by the furthest extension of the three amino acid side chains that lie closest to the heme edge, as explained in the text. [b] The three-dimensional structures of these cytochromes are not known. [c] Calculated from the structure of tuna cytochrome *c*.

proteins that might be ascribed to differing surface topologies. Examination of space-filling models of the 3-D structures of tuna and *Paracoccus* shows that three side chains project out from the surface in the region of the exposed heme edge to a greater extent in the former than in the latter. The tuna side chains are Gln-16, Val-28, and Ile-81. These are substituted by Ala, Thr, and Thr in *Paracoccus* c_2 and assume a slightly different orientation. Ile-81 is substituted by Ala in *Candida* and Val-28 by Thr in horse cytochrome *c*. The side chains nearest the exposed heme edge in *Pseudomonas* cytochrome *c*-551 are Ala-14, Val-23, and Pro-62. We measured the distance from the plane defined by the furthest extensions of the three side chains to the methyl of the substituted vinyl side chain at position 4 of the heme ring (heme β-methyl) in order to determine the extent to which they might exert a steric hindrance to the approach of a bulky reductant such as FMN. In Table III, we show that there is a clear correlation between the ratio of experimental to theoretical FMN rate constants and the distance of the heme from the protein surface (as defined above). On this basis, we predict that the 3-D structure of those cytochromes that lie close to the theoretical line in Figure 1 will have side chains near the heme edge that project out from the surface to about the same extent as in *Paracoccus* and *Rs. rubrum* cytochromes c_2, but that in *Euglena* and *Ectothiorhodospira* cytochromes the heme β-methyl will very likely protrude from the surface of the protein.

While amino acid substitutions near the exposed heme edge can apparently account for the relative reactivity of the above-mentioned cytochromes with FMN in terms of steric restriction of access to the heme, it is more difficult to explain why a similar effect is not observed with riboflavin. A possible rationalization may be that the average position of the ribityl phosphate side chain in the FMN semiquinone is constrained by interactions between the phosphate and the isoalloxazine ring (e.g., hydrogen bonding and/or electrostatic interactions with N5). In the case of riboflavin, where such interactions are absent, the side chain can assume a wider variety of orientations, which on the average can direct it further away from the protein surface during the electron-transfer interaction. Such a possibility is not unreasonable since it is known that the presence of the phosphate group in FMN decreases the redox potential and increases the semiquinone p*K* relative to lumiflavin and riboflavin (Draper & Ingraham, 1968; Vaish & Tollin, 1971), both effects being consistent with an interaction between the phosphate group and N5. The somewhat greater scatter with respect to the theoretical curve in the riboflavin data when compared with lumiflavin and the still greater nonideal behavior for the FMN reactions may be a consequence of the increasingly greater steric effects experienced by the reactants. It seems reasonable to conclude then that small differences in protein surface topologies can cause appreciable variations in rate constant only with larger and more sterically constrained reactants. We would therefore expect such effects to be even greater when other proteins are used as electron donors. That this is indeed the case will be shown in a subsequent publication.

Acknowledgments

We are grateful to Dr. R. Feldman, Division of Computer Research and Technology, National Institutes of Health, for the stereo slides of space-filling models of tuna and *Paracoccus* cytochromes *c*.

Registry No. FMN semiquinone, 34469-63-1; riboflavin semiquinone, 35919-91-6; lumiflavin semiquinone, 34533-61-4; cytochrome *c*, 9007-43-6; cytochrome c_2, 9035-43-2.

References

Agmon, N., & Levine, R. D. (1977) *Chem. Phys. Lett. 52*, 197–201.

Ahmad, I., Cusanovich, M. A., & Tollin, G. (1981) *Proc. Natl. Acad. Sci. U.S.A. 78*, 6724–6728.

Draper, R. D., & Ingraham, L. L. (1968) *Arch. Biochem. Biophys. 125*, 802–808.

Ferguson-Miller, S., Brautigan, D. L., & Margoliash, E. (1978) *J. Biol. Chem. 253*, 149–159.

Koppenol, W. H., & Margoliash, E. (1982) *J. Biol. Chem. 257*, 4426–4437.

Marcus, R. A. (1968) *J. Phys. Chem. 72*, 891–899.

Matsuura, Y., Takano, T., & Dickerson, R. E. (1982) *J. Mol. Biol. 156*, 389–409.

Matthew, J. B., Weber, P. C., Salemme, F. R., & Richards, F. M. (1983) *Nature (London) 301*, 169–171.

McArdle, J. V., Gray, H. B., Creutz, C., & Sutin, N. (1974) *J. Am. Chem. Soc. 96*, 5737.

Meyer, T. E., & Kamen, M. D. (1982) *Adv. Protein Chem. 35*, 105–212.

Meyer, T. E., Przysiecki, C. T., Watkins, J. A., Bhattacharyya, A., Simondsen, R. P., Cusanovich, M. A., & Tollin, G. (1983) *Proc. Natl. Acad. Sci. U.S.A. 80*, 6740–6744.

Miller, W. G., & Cusanovich, M. A. (1974) *Bioelectrochem. Bioenerg. 1*, 448–458.

Miller, W. G., & Cusanovich, M. A. (1975) *Biophys. Struct. Mech. 1*, 97–111.

Nagy, J., Knoll, J., Kenney, W. C., & Singer, T. P. (1982) in *Flavins and Flavoproteins* (Massey, V., & Williams, C. H., Jr., Eds.) pp 573–578, Elsevier/North-Holland, New York.

Przysiecki, C. T. (1984) Ph.D. Thesis, University of Arizona.

Rehm, D., & Weller, A. (1969) *Ber. Bunsenges. Phys. Chem. 73*, 834–839.

Rickle, G. K., & Cusanovich, M. A. (1979) *Arch. Biochem. Biophys. 197*, 589–598.

Rieder, R., & Bosshard, H. R. (1980) *J. Biol. Chem. 255*, 4732–4739.

Salemme, F. R., Kraut, J., & Kamen, M. D. (1973) *J. Biol. Chem. 248*, 7701–7716.

Simondsen, R. P., & Tollin, G. (1983) *Biochemistry 22*, 3008–3016.

Simondsen, R. P., Weber, P. C., Salemme, F. R., & Tollin, G. (1982) *Biochemistry 21*, 6366–6375.

Smith, H. T., Ahmed, A. J., & Millett, F. (1981) *J. Biol. Chem. 256*, 4984–4990.
Smith, M. B., Stonehuerner, J., Ahmed, A. J., Staudenmayer, N., & Millett, F. (1980) *Biochim. Biophys. Acta 592*, 303–313.
Staudenmayer, N., Ng, S., Smith, M. B., & Millet, F. (1977) *Biochemistry 16*, 600–604.
Timkovich, R., & Dickerson, R. E. (1976) *J. Biol. Chem. 251*, 4033–4046.
Vaish, S. P., & Tollin G. (1971) *Bioenergetics 2*, 61–72.
Van Leeuwen, J. W. (1983) *FEBS Lett. 156*, 262–264.
Watkins, J. A. (1984) Ph.D. Thesis, University of Arizona.
Wood, F. E., Post, C. B., & Cusanovich, M. A. (1977) *Arch. Biochem. Biophys. 184*, 586–595.

Phosphorothioate Analogues of 5-Phosphoribosyl 1-Diphosphate: Synthesis, Purification, and Partial Characterization†

Geoffrey W. Smithers‡ and William J. O'Sullivan*

ABSTRACT: The 1-phosphorothioate analogues of 5-phosphoribosyl 1-diphosphate (P-Rib-PP) have been prepared enzymatically, in reactions catalyzed by P-Rib-PP synthetase from *Salmonella typhimurium*. 5-Phosphoribosyl 1-*O*-(2-thiodiphosphate) (P-Rib-PPβS) was synthesized from ribose 5-phosphate (Rib-5-P) and the Mg^{2+} complex of adenosine 5′-*O*-(3-thiotriphosphate). The S_P and R_P diastereomers of 5-phosphoribosyl 1-*O*-(1-thiodiphosphate) (P-Rib-PPαS) were synthesized from Rib-5-P and the Mg^{2+} complex of adenosine 5′-*O*-(2-thiotriphosphate) (ATPβS) (S_P diastereomer, Δ-configuration) and the Cd^{2+} complex of ATPβS (R_P diastereomer, Δ-configuration), respectively. The strategy for the synthesis and stereochemical assignment of the P-Rib-PPαS diastereomers was based on the specificity of P-Rib-PP synthetase for the (Δ)-β,γ-bidentate metal–nucleotide substrate and the stereochemical course of the synthetase reaction, leading to inversion of configuration at the P_β atom of the nucleotide [Li, T. M., Mildvan, A. S., & Switzer, R. L. (1978) *J. Biol. Chem. 253*, 3918–3923], and the known configurations of the Mg^{2+} and Cd^{2+} β,γ-bidentate complexes of the ATPβS diastereomers [Jaffe, E. K., & Cohn, M. (1979) *J. Biol. Chem. 254*, 10839–10845]. The P-Rib-PP analogues were purified by gradient elution from DEAE-Sephadex and characterized by chemical analysis and ^{31}P nuclear magnetic resonance [Smithers, G. W., & O'Sullivan, W. J. (1984) *Biochemistry* (following paper in this issue)]. A preliminary account of their interaction with human brain hypoxanthine phosphoribosyltransferase and yeast orotate phosphoribosyltransferase (OPRTase) is described. The substrate activity of the analogues with OPRTase formed the basis for a specific and convenient assay based on the release of $^{14}CO_2$ from [*carboxy*-^{14}C]orotate in the presence of excess orotidylate decarboxylase, analogous to the procedure used in the determination of the parent compound. The potential application of the P-Rib-PP analogues as probes of the mechanistic basis of the phosphoribosyltransferase enzymes is discussed.

Phosphorothioate analogues of the adenosine nucleotides, particularly ATP, in which a nonbridging oxygen atom is replaced with sulfur have proved highly rewarding as probes of the mechanistic basis of enzyme-catalyzed phosphoryl group transfer reactions and other ATP-dependent processes (Eckstein, 1979, 1980, 1983; Knowles, 1980; Eckstein et al., 1982; Cohn, 1982). Important applications have included (1) studies of the chelate configuration of the metal–nucleotide substrate species at the active site of various kinases (Eckstein, 1979; Cohn, 1982) based on the preferential ligation of Cd^{2+} ions to sulfur and Mg^{2+} ions to oxygen in the phosphorothioates (Jaffe & Cohn, 1978a, 1979) and (2) the elucidation of the mechanism and stereochemical course of phosphoryl group transfer reactions, usually in combination with the ^{17}O and ^{18}O isotopes (Knowles, 1980; Eckstein et al., 1982; Frey et al., 1982; Tsai, 1982).

An extension of such applications to a study of the phosphoribosyltransferases would yield insight into the mechanism of the reactions catalyzed by this group of enzymes. Such reactions involve the transfer of the 5-phosphoribose moiety from P-Rib-PP[1] to various nitrogenous acceptor molecules and, like the kinase reactions, are absolutely dependent upon the presence of a divalent cation, usually Mg^{2+} (Musick, 1981). This requirement reflects, at least in part, the formation of a complex (or complexes) between the metal ion and the phosphooxyanion moieties of P-Rib-PP (Thompson et al., 1978; Smithers & O'Sullivan, 1982). As has been the experience with the diastereomers of ATPαS and ATPβS (Jaffe & Cohn, 1978a, 1979; Cohn, 1982), suitable sulfur-substituted analogues of P-Rib-PP should have direct application as probes of the "metal–P-Rib-PP" structure at the active site of the phosphoribosyltransferase enzymes.

† From the School of Biochemistry, University of New South Wales, Kensington, New South Wales 2033, Australia. *Received November 1, 1983.* This work was supported, in part, by financial assistance from the Australian Research Grants Scheme.

‡ Supported by a Commonwealth postgraduate research scholarship. Present address: Department of Biochemistry and Biophysics, University of Pennsylvania School of Medicine, Philadelphia, PA 19104.

[1] Abbreviations: P-Rib-PP, 5-phosphoribosyl 1-diphosphate; ATPαS, adenosine 5′-*O*-(1-thiotriphosphate); ATPβS, adenosine 5′-*O*-(2-thiotriphosphate); P-Rib-PPβS, 5-phosphoribosyl 1-*O*-(2-thiodiphosphate); ATPγS, adenosine 5′-*O*-(3-thiotriphosphate); P-Rib-PPαS, 5-phosphoribosyl 1-*O*-(1-thiodiphosphate); HPRTase, hypoxanthine phosphoribosyltransferase; OPRTase, orotate phosphoribosyltransferase; NMR, nuclear magnetic resonance; ADPβS, adenosine 5′-*O*-(2-thiodiphosphate); Mes, 4-morpholineethanesulfonic acid; Hepes, 4-(2-hydroxyethyl)-1-piperazineethanesulfonic acid; PEI, poly(ethylenimine); DEAE, diethylaminoethyl; ODCase, orotidylate decarboxylase; EDTA, ethylenediaminetetraacetic acid; HPLC, high-performance liquid chromatography; TLC, thin-layer chromatography; P_i, inorganic phosphate; P-Rib-PP(S), 1-phosphorothioate analogue of P-Rib-PP; SPP_i, thiopyrophosphate.

0006-2960/84/0423-4767$01.50/0